

***In vitro* effects of 2-methoxyestradiol-bis-sulphamate on cell growth, morphology and cell cycle dynamics in the MCF-7 breast adenocarcinoma cell line**

CHRIS VORSTER, ANNIE JOUBERT

Department of Physiology, University of Pretoria, P.O. Box 2034, Pretoria, 0001, South Africa

Key words: cancer, 2-methoxyestradiol, sulphamoylated estradiol derivative, apoptosis, autophagy

ABSTRACT: In the search for new and improved anticancer therapies, researchers have identified several potentially useful compounds. One of these agents is 2-methoxyestradiol-bis-sulphamate (2ME-BM), a sulphamoylated derivative of 2-methoxyestradiol. The objective of this study was to evaluate 2ME-BM's *in vitro* efficacy as antiproliferative agent in the MCF-7 breast adenocarcinoma cell line. Light- and fluorescent microscopy showed decreased cell density, increased apoptotic characteristics and significant ultrastructural aberrations indicative of autophagic cell death after 24 hours of exposure at a concentration of 0.4 μ M. In addition, mitotic indices revealed that 2ME-BM induces a G₂M block. The latter was confirmed by flow cytometric analyses where increased sub-G₁ and G₂/M fractions, as well as an increase in cyclin B1 levels were observed. Further *in vitro* research into the mechanism of this potentially useful anticancer compound is thus warranted.

Introduction

It has been reported that the natural metabolite of estradiol, namely 2-methoxyestradiol (Fig. 1), is a mitogen antagonist and tubulin poison that hinders cell proliferation and induces apoptosis in a diversity of non-tumor and tumor cell lines *in vitro* and suppresses growth in certain murine tumors *in vivo* (Nakagawa-Yagi *et al.*, 1996; Klauber *et al.*, 1997; Wang *et al.*, 2000; Mooberry, 2003a,b; Hait *et al.*, 2007; Sutherland *et al.*, 2007). In addition, this 17- β -estradiol derivative has been shown to exert anti-inflammatory and anti-angiogenic effects (Attalla *et al.*, 1996; Mooberry, 2003a). 2-Methoxyestradiol implements its antimitotic effects regardless of the cell's hormone receptor status

and is accountable for abnormal mitotic spindle formation and mitotic accumulation in both estrogen receptor (ER) positive- and ER negative cells (Nakagawa-Yagi *et al.*, 1996; Wang *et al.*, 2000; Mooberry, 2003a). Possible molecular targets of 2-methoxyestradiol include hypoxia-inducible factor-1 α (HIF-1 α), mammalian target of rapamycin (mTOR) and tubulin. HIF-1 α is a subunit of HIF-1, a transcription factor which is normally activated during hypoxia to facilitate transcription of genes involved in angiogenesis, oxygen transport, glucose metabolism, growth factor signaling, apoptosis, invasion and metastasis (Bárdos and Ashcroft, 2005). mTOR is a protein kinase influenced by the nutritional environment of the cell, growth factors (endothelial growth factor (EGF), insulin-like growth factor (IGF)) and stress hypoxia. mTOR regulates the rate of protein synthesis (and thus cell growth), cyclin-dependent kinase synthesis, HIF-1 activation and cytoskeletal organization (Strimpakos *et al.*, 2009).

*Address correspondence to: Annie Joubert.

E-mail: annie.joubert@up.ac.za

Received: February 22, 2010. Revised version received: May 28, 2010. Accepted: June 12, 2010.

Since certain clinical trials have shown 2-methoxyestradiol to be orally active and well tolerated, was subsequently included in human phase II clinical trials against breast cancer, prostate cancer and in patients suffering from multiple myeloma, renal cell carcinoma, as well as rheumatoid arthritis (Lakhani *et al.*, 2003; James *et al.*, 2006).

Hitherto, several studies have increased our knowledge of how 2-methoxyestradiol exerts its pleiotropic effects; however, the molecular mechanisms of action are not yet elucidated. Accordingly, 2-methoxyestradiol has manifested itself as a potential anticancer agent (Mooberry, 2003b) and current research aims to refine the structures surrounding the steroid nucleus of the molecule to provide higher efficacy and lower toxicity (Mooberry, 2003b). Newman *et al.* (2006) showed that bioavailability was among the parameters which could be improved by sulphamoylation of 2-methoxyestradiol (Raobaikady *et al.*, 2003; Chander *et al.*, 2007).

Among these derivatives is 2-methoxyestradiol-bis-sulphamate (2ME-BM) (Fig. 1), a sulphamoylated analogue originally developed as a steroid sulphatase inhibitor (Purohit *et al.*, 1998). Steroid sulphatase inhibitors are intended to target hormone-dependent cancers by interfering with the conversion of estrone sulphate to estrone and the hydrolysis of dehydroepiandrosterone sulphate to dehydroepiandrosterone, which is reduced to 5-androstenediol (Purohit *et al.*, 2003). 2ME-BM has been shown to possess higher oral bioavailability when compared to 2-methoxyestradiol (Suzuki *et al.*, 2003; Ireson *et al.*, 2004; Utsumi *et al.*, 2005). This characteristic is possibly related to the sulphamate group added to the original 2-methoxyestradiol molecule. While 2ME-BM irreversibly inhibits cancer cell proliferation and tumor growth (Purohit *et al.*, 1998; Suzuki *et al.*, 2003; Ireson *et al.*, 2004; Utsumi *et al.*, 2005; James *et al.*, 2006) in both *in vitro* and *in vivo* studies (Foster *et al.*, 2008) in

breast cancer models of both ER positive and negative tumors, as well as multiple drug resistant (MDR) cell lines (Suzuki *et al.*, 2003), the intracellular events responsible for these effects are poorly characterized. In view of the enhanced potencies associated with sulphamoylated 2-methoxyestradiol derivatives in traditionally resilient ER α -negative cells, these analogues hold considerable therapeutic potential for the treatment of both hormone-dependent and hormone-independent breast cancers.

The aim of this study was thus to evaluate the *in vitro* effects exerted by 2ME-BM in the MCF-7 breast adenocarcinoma cell line with regard to cell growth, morphology and cell cycle dynamics in order to contribute to the elucidation of the *in vitro* signal transduction effects exerted by 2ME-BM.

Materials and Methods

Cell line

The MCF-7 cell line is derived from a pleural effusion of human breast adenocarcinoma which is commercially available from Highveld Biological Pty. (Ltd.) (Sandringham, South Africa).

Materials

The fluorescein-isothiocyanate conjugated cyclin B1 antibody reagent set was obtained from BD Pharmingen (Rockville, United States of America). Unless otherwise specified, all other analytical grade reagents were obtained from Sigma (St. Louis, United States of America) or Highveld Biological (Pty) Ltd. (Sandringham, South Africa).

Drug synthesis

Since 2ME-BM is not commercially available the estradiol-bis-sulphamate precursors and 2ME-BM were synthesized by Prof. R. Vlegaar from the Department of Chemistry at the University of Pretoria (Pretoria, South Africa).

Cell culture

MCF-7 cells were cultured in Dulbecco's Modified Eagle's Medium (DMEM) supplemented with 10% fetal bovine serum (FCS), penicillin (100 μ g/l), streptomycin (100 μ g/l) and fungizone (250 μ g/l) at 37°C in a 5% carbon dioxide environment. After seeding of an

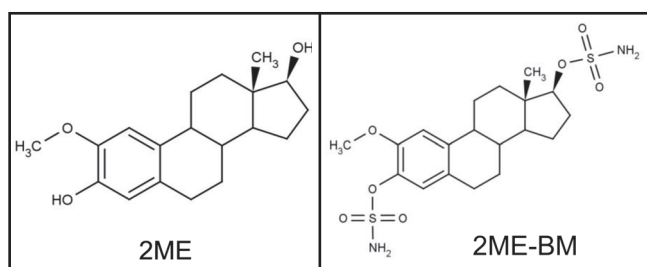


FIGURE 1. Chemical structure of 2-methoxyestradiol and 2ME-BM (drawings by authors using Marvin Sketch software available from ChemAxon at http://www.chemaxon.com/product/marvin_land.html.)

appropriate number of cells, flasks and plates were left overnight to allow for cell attachment. All experiments included vehicle control samples in the form of cells propagated in growth medium only (MO), cells exposed to equivalent amounts of the vehicle dimethyl sulphoxide (DMSO), as well as positive controls for apoptosis (actinomycin D) and autophagy (cells starved by culturing in 20% medium and 80% phosphate buffered saline). The DMSO vehicle has been shown to be non-toxic at the concentrations utilized (0.01% - 0.04% v/v) and no statistically significant effects were observed in any of the tests conducted for this study when vehicle control samples were compared to samples propagated in growth medium. For each experiment, culture medium was changed before exposure.

Cell numbers (crystal violet staining)

Time-(24, 48, 72 hours) and dose-(0.2 μ M - 1 μ M) dependent cell proliferation studies were conducted in order to determine the optimal dosage of 2ME-BM for inhibition of cell proliferation and to select the optimal exposure parameters for this specific study. The experimental parameters were chosen to reflect previously utilized concentrations and exposure times (Suzuki *et al.*, 2003; Raobaikady *et al.*, 2003; Utsumi *et al.*, 2005). Cells were seeded at 5 000 cells per well in 96-well plates and incubated overnight to ensure attachment. Cells were subsequently exposed to different concentrations of 2ME-BM for 24, 48 and 72 hours, after which the experiment was terminated by removal of the medium and subsequent fixation of cells by glutaraldehyde. After 15 minutes, glutaraldehyde was replaced by crystal violet and cells were stained for a further 30 minutes. The plates were washed under slowly running tap water to remove excess stain and left to dry overnight. Crystal violet was then solubilized by addition of 200 μ l of Triton-X100 and incubation at room temperature for 30 minutes. After mixing, 100 μ l of the solution was transferred to a clean 96-well plate and the absorbance was determined using a Bio-Tek Instruments ELX-800 Universal Microplate Reader (Winooski, United States of America). Baseline values were determined before exposure to 2ME-BM in order to quantify starting cell numbers. After half maximal inhibitory concentration (IC₅₀) values were calculated, it was decided to continue all subsequent experiments using an exposure time of 24 hours and 0.4 μ M 2ME-BM, since these parameters presented the most significantly differential results in MCF-7 cells when compared to the non-tumorigenic MCF-12A breast epithelial cell line (data not shown).

Differential Interference Contrast Microscopy

Differential interference microscopy (DIC) was used to non-invasively evaluate the qualitative status of cell populations. This technique utilizes a beam of polarized light being split into two beams, polarized at 90° to each other with each taking a slightly different path through the sample. The optical density of the sample causes these two beams to interfere with each other before they are recombined. The result is a three-dimensional relief indicating variations in optical density of the sample. DIC photomicrographs were taken of cells prior to fixation for haematoxylin and eosin staining using a Zeiss inverted Axiovert CFL40 microscope and a Zeiss Axiovert MRm monochrome camera (Carl Zeiss MicroImaging, Inc., New York, United States of America).

Hematoxylin and eosin staining

Hematoxylin and eosin cell staining was conducted as a standard microscopic technique for qualitative evaluation of cellular morphology and in order to calculate the mitotic indices for quantitation of the cell cycle phase shift and abnormal morphology. Cells were seeded on heat-sterilized coverslips at 250 000 cells per well in 6-well plates and allowed to attach overnight. Cells were then exposed to 0.4 μ M 2ME-BM and appropriate controls respectively for 24 hours, after which coverslips were removed and fixed with Bouin's fixative for 30 minutes and 70% ethanol for a further 20 minutes. Coverslips were rinsed with tap water, stained with hematoxylin for 20 minutes, rinsed with tap water and 70% ethanol and stained with eosin for 7 minutes. Coverslips were dehydrated stepwise with ethanol (70%, 96%, 100%) and xylene, mounted on microscope slides using entellan resin and were allowed to dry overnight. Qualitative evaluation was conducted at 100x and 400x magnification with a Zeiss inverted Axiovert CFL40 microscope and photomicrographs were taken with a Zeiss Axiovert MRm monochrome camera (Carl Zeiss MicroImaging, Inc., New York, United States of America). Mitotic indices were performed by microscopic examination of slides prepared for hematoxylin and eosin light microscopy in order to quantify the observed effects. Cells were divided into the different phases of the cell cycle based on cellular and nuclear morphology. Where cells could not be categorized due to excessive fragmentation, highly unusual nuclear morphology or lack of clear nuclear material they were defined and counted as abnormal. Cells (1000) in total

were counted per slide and data was converted to represent the percentages of cells in each defined category.

Fluorescent microscopy

A fluorescent dye staining method was utilized in order to determine the effect that 2ME-BM has on acidic vesicular organelle formation. Acridine orange is a lysosomotropic fluorescent compound that serves as a tracer for acidic vesicular organelles including autophagic vacuoles and lysosomes. Cells undergoing autophagy will have an increased tendency for acridine orange staining when compared to viable cells. Hoechst 33342 is a fluorescent dye that can penetrate intact cell membranes of viable cells and cells undergoing apoptosis and stains the nucleus. Cells were seeded at 250 000 cells per well in 6-well plates and allowed to attach overnight. Cells were subsequently exposed to 2ME-BM and appropriate controls respectively for 24 hours and incubated with 0.9 μ M Hoechst 33342 and 50 μ M acridine orange for 30 minutes at 37°C. Subsequently, 12 μ M propidium iodide (PI) was added for a further 5 minutes, after which the cells were washed twice with PBS. Wells were examined under a Zeiss inverted Axiovert CFL40 microscope and photomicrographs were taken with a Zeiss Axiovert MRm monochrome camera (Carl

Zeiss MicroImaging, Inc., New York, United States of America) using different fluorescence filters to distinguish between the stains. Images were composited with Zeiss AxioVision software. Zeiss Filter 2 was used for Hoechst 33342 (blue emission)-stained cells and Zeiss Filter 9 for acridine orange-stained (green emission) cells.

Transmission Electron Microscopy

Transmission electron micrographs were acquired in order to examine the ultrastructural changes associated with 2ME-BM exposure. Cells were seeded at 750 000 cells per flask in 25cm² flasks and allowed to attach overnight. Cells were subsequently exposed to 2ME-BM and appropriate controls respectively for 24 hours, fixed and embedded according to standard transmission electron microscopy procedures (glutaraldehyde, osmium tetroxide, ethanol dehydration, quetol embedding) (Hayat *et al.*, 1981) at the University of Pretoria's Microscopy Unit (Pretoria, South Africa). Sections were cut using a diamond ultramicrotome and placed on copper grids. Samples were further contrasted with aqueous uranyl acetate and Reynolds lead citrate before electron micrographs were taken at the University of Pretoria's Onderstepoort campus Microscopy Unit (Pretoria, South Africa).

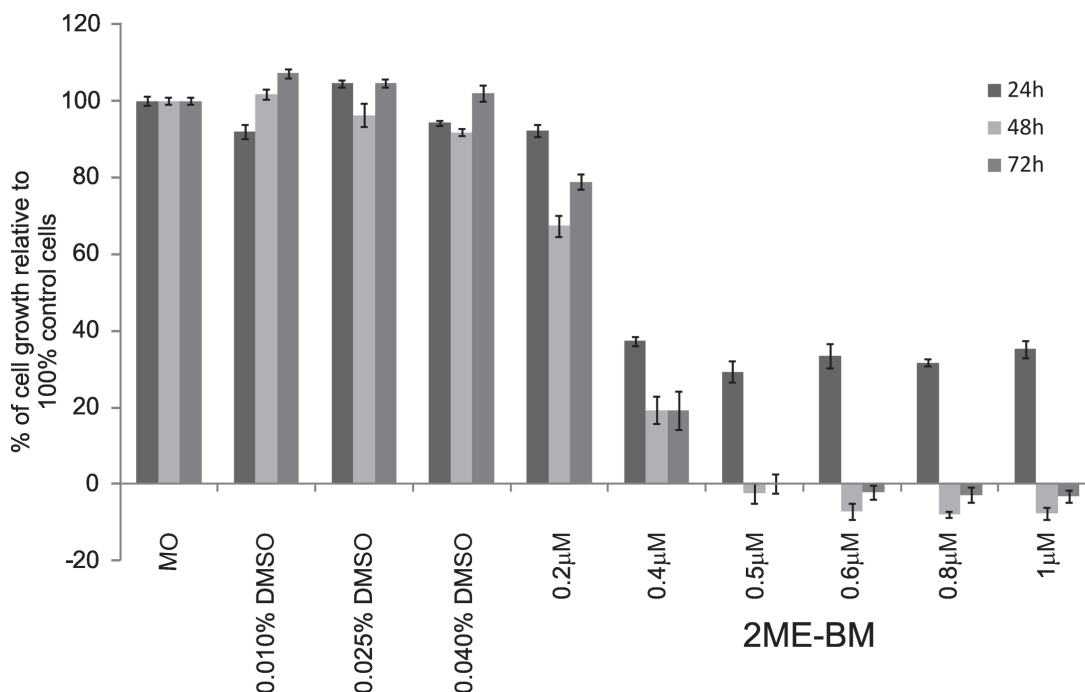


FIGURE 2. Crystal violet assays conducted utilizing a concentration series of 2ME-BM (0.2 μ M - 1.0 μ M) and three different exposure times (24 hours, 48 hours and 72 hours). Appropriate controls were included. A significant decline in GI₅₀ values was observed between 0.2 μ M and 0.4 μ M after 24 hours of 2ME-BM exposures. GI₅₀ values were calculated from the spectrophotometrical data using the standard formula: $(\text{test} - \text{baseline}) / (\text{control} - \text{baseline}) \times 100 = \text{GI}_{50}$ value.

Flow cytometry

Flow cytometry was used to confirm the observed cell cycle disturbances and to investigate the intracellular events causing these aberrations. Cells were seeded at 750 000 cells per flask in 25cm² flasks and allowed to attach overnight. Cells were exposed to 2ME-BM and appropriate controls respectively for 24 hours, after which cells were trypsinized and fixated with 10 ml ice-cold 70% ethanol and stored at 4°C for 24 hours. After 24 hours, cells were trypsinized and washed with PBS. Cells (1x10⁶) were incubated with either the isotypic control (isothiocyanate-conjugated mouse immunoglobulin G (IgG), or the isothiocyanate-conjugated anti-cyclin B1 antibody for 30 min at room temperature. Cells were washed and resuspended in 0.5 ml PBS containing 40 µg/ml propidium iodide and 100 µg/ml RNase A for 30 min at 4°C. Propidium iodide staining was added in order to simultaneously analyze DNA-based cell cycle dynamics. Analyses were conducted using a Beckman Coulter Cytomics FC500 instrument (Beckman Coulter Inc., Fullerton, CA, United States of America). Data from at least 10 000 cells were analyzed with CXP software (Beckman Coulter South Africa (Pty) Ltd). Aggregated and aneuploid cells were removed from analysis by visual inspection, with sub-G₁ indicating cells with less nuclear content than normal and cellular fragments, while abnormal cells were defined as cells with more than 2N genetic content. For cyclin B1 analyses, fluorescence of the isothiocyanate-conjugated isotypic control was normalized to 1% on an FL1-lin histogram. Measurement of isothiocyanate-conjugated cyclin B1 fluorescence of control and exposed MCF-7 cells were measured utilizing the normalized area of an FL3-log vs FL1-lin dot-plot. For cell cycle analyses, results are

expressed as percentage of the cells in each phase. Generated data were analysed using Cyflogic software (CyFlo Ltd. - <http://www.cyflogic.com/>).

Statistical Analysis

Data from three independent experiments (each conducted in six replicates for crystal violet experiments) were analyzed. Representative data are shown. Quantitative data were statistically analyzed for significance using the analysis of variance (ANOVA)-single factor model followed by a two-tailed Student's *t*-test. Means are presented in bar charts, with T-bars referring to standard deviations. *P*-values < 0.05 were regarded as statistically significant. For flow cytometric data at least 10 000 events were counted per sample and percentages were calculated by gating the supplier-provided isotypic control to < 1%.

Results

Cell numbers

The crystal violet assay is a method for spectrophotometrically detecting the number of cells in a specific sample by measuring dye uptake by DNA. Results show a time-and dose-dependent decrease in cell numbers with exposure to 2ME-BM (Fig. 2). A concentration of 0.4µM 2ME-BM and exposure time of 24 hours were selected as the optimal time and dose, since these conditions inhibited cell growth with 50% (GI₅₀ value). The GI₅₀ was determined by calculating the drug concentration at which the control sample showed a 50% increase in growth above the test sample, taking into

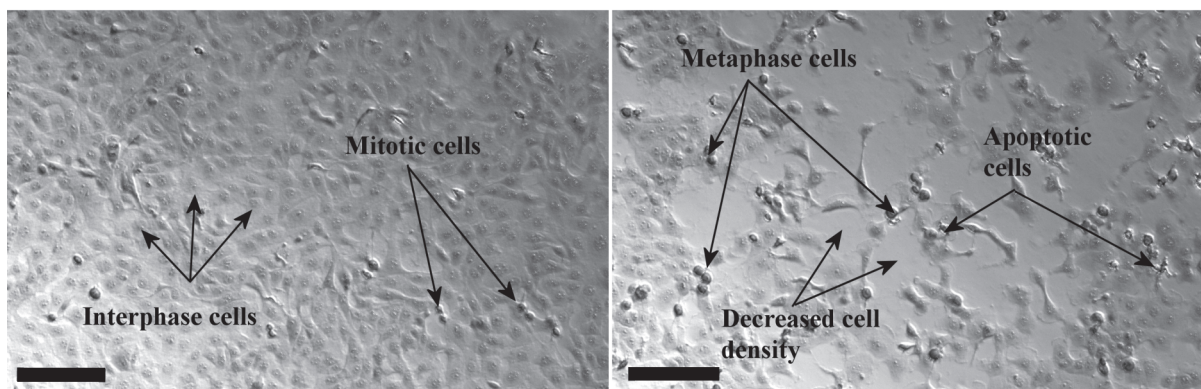


FIGURE 3. Differential interference contrast microscopy examination of samples before termination for hematoxylin and eosin staining. A significant decrease in cell density, changes in morphology and an increased amount of cellular debris in the 2ME-BM-exposed cells was observed. Scale bar represents 100µm.

account the number of cells in each sample at the time of exposure. All subsequent studies were conducted using these experimental parameters.

DIC microscopy

A decrease in cell numbers and density in samples exposed to 2ME-BM was observed when compared to vehicle control (DMSO) samples (Fig. 3). An increased number of cells in metaphase (round cells) and apoptosis (fragmented, hypercondensed chromatin) were visible.

Hematoxylin and eosin staining

Qualitative analysis by means of hematoxylin and eosin staining revealed a sharp decrease in cell density and significant morphological changes with 2ME-BM exposure (Fig. 4). Apoptotic cells (condensed nuclei, cytoplasmic blebbing) and cells blocked in metaphase were observed. Quantitative analyses by means of mitotic indices showed a distinct increase in the number of apoptotic and abnormal cells in samples exposed to 2ME-BM, as well as well-defined perturbations of mi-

totic dynamics (Fig. 5). One thousand cells were counted per slide and numbers were converted to percentages. A large increase in the number of cells in metaphase was observed. Nearly no cells progressed further than metaphase in treated samples.

Fluorescent microscopy

In addition to confirming the marked decrease in cell density and increase in metaphase cells, fluorescent triple-staining revealed an increase in the amount of acidic intracellular vacuoles in 2ME-BM-treated samples when compared to vehicle control samples (Fig. 6).

Transmission Electron Microscopy

Transmission electronmicroscopy showed evidence of both apoptotic and autophagic processes occurring in cells exposed to 2ME-BM (Fig. 7). Membrane blebbing, hypercondensed chromatin, fragmented nuclei and autophagic lysosomes were observed in samples exposed to 2ME-BM.

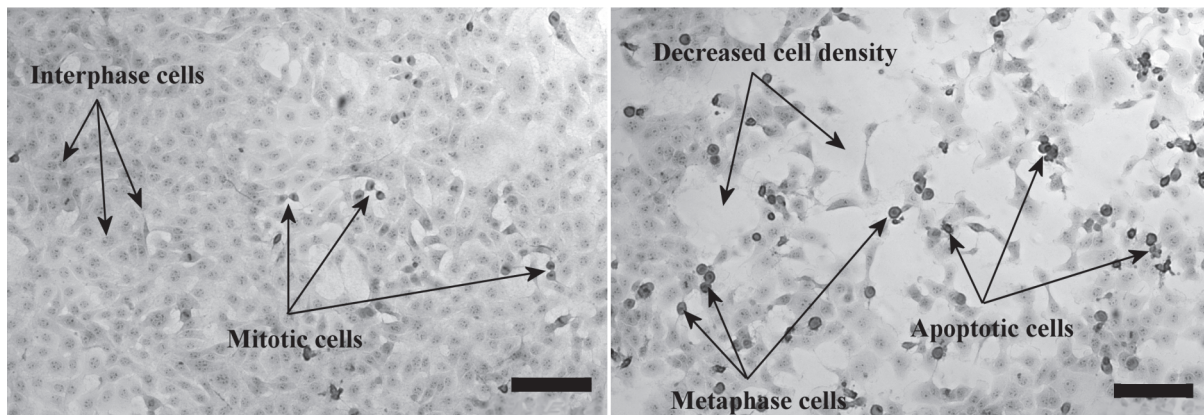


FIGURE 4. Hematoxylin and eosin staining revealed decreased cell density and increased cellular debris in addition to an increase in the amount of cells in metaphase and apoptotic cells. Scale bar represents 100µm.

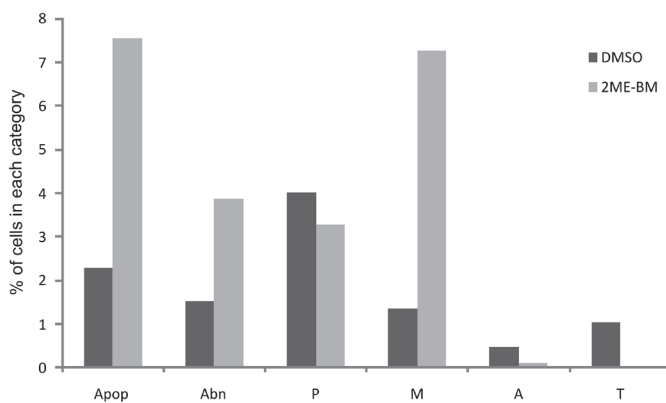


FIGURE 5. Mitotic indices were determined by examining samples prepared for hematoxylin and eosin photomicrographs using a standard light microscope. Cells were divided into the following categories: interphase (not shown), apoptotic (Apop), abnormal (Abn), prophase (P), metaphase (M), anaphase (A) and telophase (T). Abnormal cells were defined as cellular fragments or cells with no discernable nuclear morphology. Percentage of cells in each category for 2ME-BM- and vehicle control (DMSO)-exposed cells are shown with 1000 cells being counted per slide.

Flow cytometry

Flow cytometric analysis of cell cycle dynamics revealed a significant increase in the G₂/M-phase and sub-G₁ (apoptotic cellular fragment) cell fractions. This confirms previous data (PlasDIC microscopy, H&E

staining) indicating that 2ME-BM causes metaphase arrest and subsequent apoptosis. PI fluorescence was analyzed and results are represented as histograms (FL3 Lin) and percentages (Fig. 8). Analysis of intracellular cyclin B1 levels showed a 6% increase (when compared to vehicle control samples) in response to exposure to

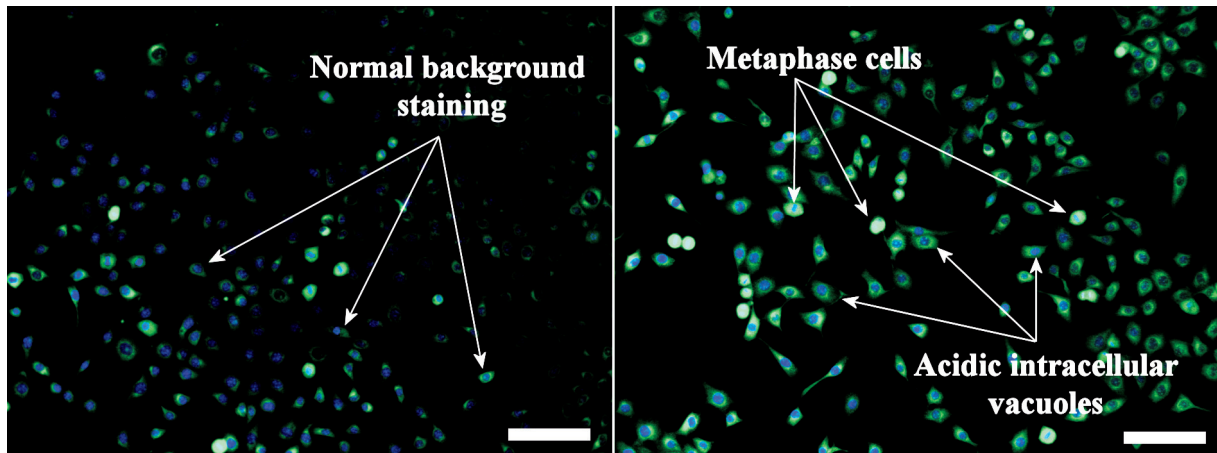


FIGURE 6. Fluorescent photomicrographs of cells stained with acridine orange showed increased intracellular acidic vesicles in 2ME-BM-exposed cells indicative of autophagy (green emission). Cells were triple stained with acridine orange, Hoechst 33342 and propidium iodide (blue emission). Scale bar represents 100µm.

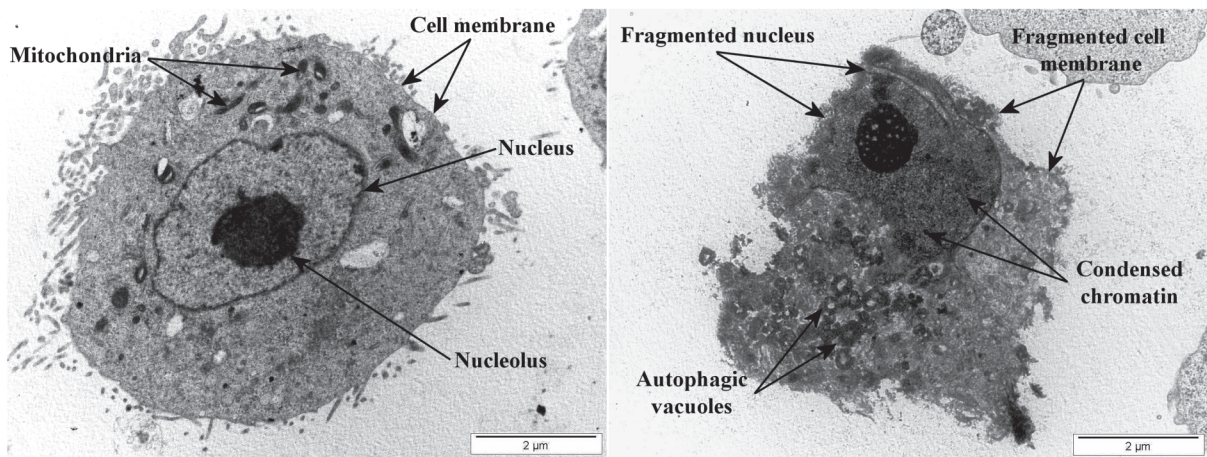


FIGURE 7. Transmission electron microscopy of cellular ultrastructure revealed significant changes in 2ME-BM-exposed cells, with the observation of apoptotic characteristics (condensed or fragmented nuclei, apoptotic bodies) and indications of autophagy (intracellular autophagosomes or vesicles).

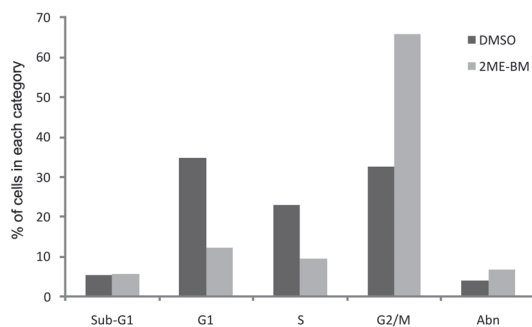


FIGURE 8. Flow cytometric analysis of cell cycle dynamic showed an increase in the sub-G₁-, abnormal and G₂/M-phase cells in 2ME-BM-exposed cells. The presence of a sub-G₁ fraction indicated cells with less nuclear content than normal and cellular fragments, while abnormal cells were defined as cells with more than 2N genetic content.

2ME-BM (Fig. 9). Gating was conducted at a positive rate of 1% for isotopic control samples. Results are expressed as histograms of FL1 Log.

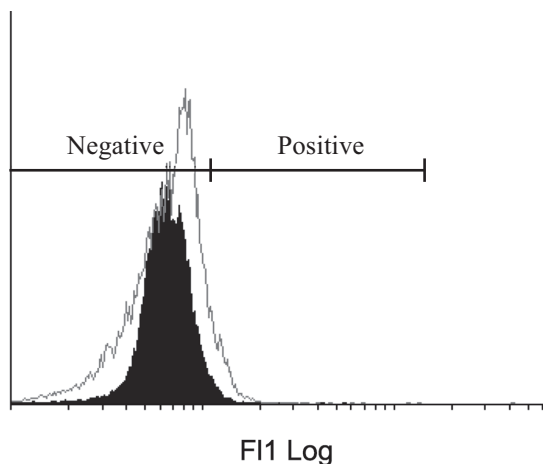


FIGURE 9. Flow cytometry revealed a significant (6%) increase in cyclin B₁ levels in exposed samples. The vehicle control sample was indicated as the solid grey area, with 2ME-BM-treated sample shown as dark grey line.

Discussion

In addition to the novel insights into the cellular mechanism of action of 2ME-BM's effects offered by these results (cell cycle analysis, autophagy detection, cyclin B1 levels), 2ME-BM was found to potently inhibit cell proliferation in a time- and dose-dependent manner in concurrence with previous studies (where 2ME-BM concentrations of 0.05–10 μ M and exposure times of up to 5 days were utilized) (Ho *et al.*, 2003; Utsumi *et al.*, 2005). This may possibly be attributed to its ability to bind to the colchicine binding site of tubulin, which would prevent chromosomal separation during mitosis. After exposure of cells to a series of 2ME-BM concentrations for 24, 48 and 72 hours, 0.4 μ M of 2ME-BM and 24 hour exposure were chosen as concentration and exposure time to be utilised for further testing. A significant decrease in cell density and growth inhibition was observed. Unlike 2-methoxyestradiol, however, this inhibition of cell division was shown to be irreversible up to 72 hours after initial exposure.

A significant shift in cell cycle progression was observed after 2ME-BM exposure, with more cells becoming trapped in the G₂/M phase transition (with cyclin B1 accumulation) and nearly no cells progressing beyond metaphase and into the subsequent mitotic phases. This effect has also been observed in other *in vitro* studies with both 2ME and 2ME-BM in HUVEC human

fibroblasts and human umbilical vein endothelial cells, LNCaP prostate carcinoma cells, androgen-independent PC3 prostate carcinoma cells and A2780 ovarian carcinoma cell line (Ho *et al.*, 2003). Under normal circumstances, cyclin B1 forms complexes with Cdk-1 (p34 kinase) generating the mitosis-promoting factor, which is held in an inactive state by phosphorylation by Wee1 kinase and Myt1 kinase. Activation is achieved through the dephosphorylation of the complex by Cdc25C. Mitosis can only progress past metaphase once the mitosis-promoting factor has been dephosphorylated and translocated to the nucleus via the microtubule network and centrosomes. Analysis of cyclin B1 showed a distinct increase in intracellular levels, possibly due to inhibition of the normal proteasomal degradation or 2ME-BM-induced defects in microtubule dynamics. Rising cyclin B1 levels in conjunction with pre-mitotic cell cycle arrest would thus indicate an upstream cell cycle machinery blockade, which warrants further investigation.

Morphology was severely affected by 2ME-BM, as observed by means of various microscopic techniques. Cell density was compromised with an increase in the number of rounded and/or visibly damaged cells. The clear increase in the number of acidic intracellular lysosomes indicated the involvement of autophagic processes, while the increased amount of cellular fragments, blebbing cells and formation of apoptotic bodies implicated apoptosis in the mechanisms of cell death.

In conclusion, this study has revealed novel insights into the intracellular events which render 2ME-BM a potent inhibitor of MCF-7 breast adenocarcinoma cell growth by demonstrating previously undocumented effects of 2ME-BM-induced cell cycle arrest and subsequent cell death through both apoptotic and autophagic processes. Given the therapeutic potential of 2ME-BM, further research into these mechanisms is warranted.

Acknowledgements

This research was supported by grants from the Medical Research Council of South Africa (AK076; AL343), the Cancer Association of South Africa (AK246), the National Research Foundation of South Africa (AL239) and the Struwig-Germeshuysen Cancer Research Trust of South Africa (AN074). The authors would like to thank the Departments of Physiology, Pharmacology and Chemistry of the University of Pretoria, as well as the University of Pretoria's Microscopy Unit (Pretoria, South Africa) for the use of their facilities and expertise.

References

- Attalla H, Makela T, Adlercreutz H, Andersson L (1996). 2-Methoxyestradiol arrests cells in mitosis without depolymerizing tubulin. *Biochemical and Biophysical Research Communications* **228**: 467-473.
- Bárdos J, Ashcroft M (2005). Negative and positive regulation of HIF-1: A complex network. *Biochimica et Biophysica Acta* **1755**: 107-120.
- Chander S, Foster P, Leese M, Newman S, Potter B, Purohit A (2007). *In vivo* inhibition of angiogenesis by sulphamoylated derivatives of 2-methoxyoestradiol. *British Journal of Cancer* **96**: 1368-1376.
- Foster P, Ho Y, Newman S, Kasprzyk P, Leese M, Potter B (2008). 2-MeOE2bisMATE and 2-EtE2bisMATE induce cell cycle arrest and apoptosis in breast cancer xenografts as shown by a novel *ex vivo* technique. *Breast Cancer Research and Treatment* **111**: 251-260.
- Hait W, Rubin E, Alli E, Goodin S (2007). Tubulin Targeting Agents. *Update on Cancer Therapeutics* **2**: 1-18.
- Hayat M (1981). *Biological Applications - Principles and techniques of electron microscopy* (Vol. 1). University Park Press, Baltimore.
- Ho Y, Newman S, Purohit A, Leese M, Potter B, Reed M (2003). The effects of 2-methoxy oestrogens and their sulphamoylated derivatives in conjunction with TNF- α on endothelial and fibroblast cell growth, morphology and apoptosis. *Journal of Steroid Biochemistry and Molecular Biology* **86**: 189-196.
- Ireson C, Chander S, Purohit A, Perera S, Newman S, Parish D (2004). Pharmacokinetics and efficacy of 2-methoxyoestradiol and 2-methoxyoestradiol-bis-sulphamate *in vivo* in rodents. *British Journal of Cancer* **90**: 932 - 937.
- James J, Murry D, Treston A, Storniolo A, Sledge G, Sidor C (2006). Phase I safety, pharmacokinetic and pharmacodynamic studies of 2-methoxyestradiol alone or in combination with docetaxel in patients with locally recurrent or metastatic breast cancer. *Investigational New Drugs* **25**: 41-48.
- Klauber N, Parangi S, Flynn E, Hamel E, D'Amato R (1997). Inhibition of angiogenesis and breast cancer in mice by the microtubule inhibitors 2-methoxyestradiol and taxol. *Cancer Research* **57**: 81-86.
- Lakhani N, Sarkar M, Venitz J, Figg W (2003). 2-Methoxyestradiol, a promising anticancer agent. *Pharmacotherapy* **23**: 165-172.
- Mooberry S (2003a). Mechanism of action of 2-methoxyestradiol: new developments. *Drug Resistance Updates* **6**: 355-361.
- Mooberry S (2003b). New insights into 2-methoxyestradiol, a promising antiangiogenic and antitumor agent. *Current Opinion in Oncology* **15**: 425-430.
- Nakagawa-Yagi Y, Ogane N, Inoki Y, Kitoh N (1996). The endogenous estrogen metabolite 2-methoxyestradiol induces apoptotic neuronal cell death *in vitro*. *Life Sciences* **58**: 1461-1467.
- Purohit A, Vernon K, Wagenaar Hummelinck A, Woo L, Hejaz H, Potter B (1998). The development of A-ring modified analogues of oestrone-3-O-sulphamate as potent steroid sulphatase inhibitors with reduced oestrogenicity. *Journal of Steroid Biochemistry and Molecular Biology* **64**: 269-275.
- Purohit A, Woo L, Chander S, Newman S, Ireson C, Ho Y (2003). Steroid sulphatase inhibitors for breast cancer therapy. *Journal of Steroid Biochemistry and Molecular Biology* **86**: 423-432.
- Raobaikady B, Purohit A, Chander S, Woo L, Leese M, Potter B (2003). Inhibition of MCF-7 breast cancer cell proliferation and *in vivo* steroid sulphatase activity by 2-methoxyoestradiol-bis-sulphamate. *Journal of Steroid Biochemistry and Molecular Biology* **84**: 351-358.
- Strimpakos A, Karapanagiotou E, Saif M, Syrigos K (2009). The role of mTOR in the management of solid tumors: An overview. *Cancer Treatment Reviews* **35**: 148-159.
- Sutherland T, Anderson R, Hughes R, Altmann E, Schuliga M, Ziogas J (2007). 2-Methoxyestradiol – a unique blend of activities generating a new class of anti-tumour/anti-inflammatory agents. *Drug Discovery Today* **12**: 577-584.
- Suzuki R, Newman S, Purohit A, Leese M, Potter B, Reed M (2003). Growth inhibition of multi-drug-resistant breast cancer cells by 2-methoxyoestradiol-bis-sulphamate and 2-ethyloestradiol-bis-sulphamate. *Journal of Steroid Biochemistry & Molecular Biology* **84**: 269-278.
- Utsumi T, Leese M, Chander S, Gaukroger K, Purohit A, Newman S (2005). The effects of 2-methoxyoestrogen sulphamates on the *in vitro* and *in vivo* proliferation of breast cancer cells. *Journal of Steroid Biochemistry & Molecular Biology* **94**: 219-227.
- Wang H, Myc A, Koenig R, Bretz J, Arscott P, Baker J (2000). 2-Methoxyestradiol, an endogenous estrogen metabolite, induces thyroid cell apoptosis. *Molecular and Cellular Endocrinology* **165**: 163-172.

